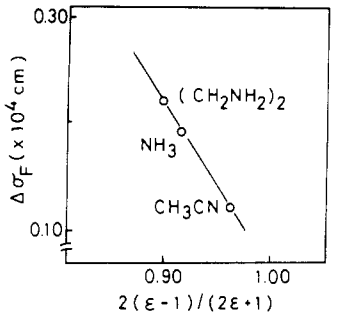

Figure 6. Relationship between the dielectric constant of adsorbates and the shift of emission peaks for Eu^{2+}–adsorbed molecule in mordenite.

Table IV. Rate Constants for Radiative (K_f) and Radiationless (K_i) Transitions

adsorbate	K_f, s^{-1}	Q_0, %	K_i, s^{-1}
none	8.2×10^3	0.9	9.0×10^5
CH_3CN	3.6×10^9	0.002	1.8×10^8
NH_3	2.0×10^5	0.2	1.0×10^8
$(CH_2NH_2)_2$	2.3×10^5	1.8	1.3×10^7

negative and $\mu_a > 0$, μ_a is always larger than μ_g. However, the slopes for Eu^{2+}–nitrogen-donor ligands are different from that for Eu^{2+}–oxygen-donor ligands as described elsewhere.[17] In the formation of complexes, it is well-known that rare earth ions prefer oxygen- to nitrogen-donor ligands. In eq 4, a and n of an oxygen-donor molecule are close to those of nitrogen-donor molecules. Therefore, the difference of slope is due to the gap of the photoexcited process between oxygen- and nitrogen-donor molecules.

Rate Constant for Radiative and Radiationless Transitions. The information obtained from the lifetime and quantum-yield measurement enables us to calculate some of the rates of radiationless transitions. The quantum yield may be expressed as

$$Q_0 = \frac{K_f}{K_f + K_i} \tag{6}$$

where K_f is the radiative rate constant and K_i is the radiationless rate constant. Also, the observed lifetime, τ, is derived from the equation

$$\tau = \frac{1}{K_f + K_i} \tag{7}$$

From eq 6 and 7, we can calculate K_f and K_i. The results are given in Table IV. The radiationless constant, K_i, increases under the gas adsorption. In a comparison of the systems of Eu^{2+}–CH_3CN, Eu^{2+}–NH_3, and Eu^{2+}–$(CH_2NH_2)_2$, the values of K_i are 180, 100, and 13, respectively. That is, the quenching rate constants are more sensitive to the nature of the adsorbates. The order of the quenching power is CH_3CN (39) > NH_3 (22) > $(CH_2NH_2)_2$ (13). The values in parentheses are the dielectric constants. The order associates with the magnitude of the dielectric constant for the adsorbates.

Acknowledgment. We are grateful to Prof. H. Mikawa and Dr. Y. Shirota of Osaka University for their support of the measurements of the lifetimes.

Registry No. Eu^{2+}, 16910-54-6; NH_3, 7664-41-7; $(CH_2NH_2)_2$, 107-15-3; CH_3CN, 75-05-8; mordenite, 12173-98-7.

Contribution from the Department of Chemistry, University of Virginia, Charlottesville, Virginia 22901

Seven-Vertex Phosphinohalometallacarboranes of Iron, Cobalt, and Nickel: Syntheses, Structures, and Reactions[1a]

HENRY A. BOYTER, JR., ROBERT G. SWISHER,[1b] EKK SINN, and RUSSELL N. GRIMES*

Received February 19, 1985

The reaction of the *nido*-2,3-$Et_2C_2B_4H_5^-$ ion with $(Ph_3P)_2NiBr_2$ in THF at room temperature gave purple, crystalline 1-Br-1,5-$(Ph_3P)_2$-1,2,3-$Ni(Et_2C_2B_4H_3)$ (**1**), whose phosphino ligands are attached to nickel and boron, respectively. The same carborane ion reacted with $(Ph_2PCH_2)_2$ and MCl_2 (M = Co, Fe) in THF to give the crystalline metallacarboranes 1,1-$(Ph_2PCH_2)_2$-1-Cl-1,2,3-$M(Et_2C_2B_4H_4)$ (**2**, M = Co; **3**, M = Fe). Products **1–3** were structurally characterized by single-crystal X-ray diffraction and by IR, UV–visible, and mass spectra; in addition, high-field NMR spectra were obtained for the diamagnetic species **1** and **2**, while paramagnetic **3** was examined via ESR and magnetic susceptibility measurements, which support the presence of low-spin Fe(III) in **3**. The MC_2B_4 cages in all three compounds have normal closo seven-vertex (pentagonal-bipyramidal) geometry. Although **3** has one less electron than **2**, its cage shows no significant distortion; hence, the unpaired electron appears to be localized in a nonbonding orbital on iron. The chlorine ligand in **2** was unaffected by NaH but was displaced by CN on treatment with KCN in refluxing CH_3OH, giving 1,1-$(Ph_2PCH_2)_2$-1-CN-1,2,3-$Co(Et_2C_2B_4H_4)$. The reaction of **2** with CH_3MgI gave the iodo complex 1,1-$(Ph_2PCH_2)_2$-1-I-1,2,3-$Co(Et_2C_2B_4H_4)$ as the only isolable metallacarborane product. The crystal structure determinations on **1**, **2**, and **3** are the first to be reported for metallacarboranes containing first-row transition-metal–halogen bonds. Crystal data for **1**: mol wt 792; space group $P\bar{1}$; $Z = 2$; $a = 11.115$ (4), $b = 12.497$ (5), $c = 14.358$ (8) Å; $\alpha = 90.34$ (4), $\beta = 94.57$ (4), $\gamma = 91.80$ (2)°; $V = 1987$ Å^3; $R = 0.059$ for 4741 reflections having $F_o^2 > 3\sigma(F_o^2)$. Crystal data for **2**: mol wt 622; space group $P2_1$; $Z = 2$; $a = 8.311$ (2), $b = 15.357$ (3), $c = 12.635$ (5) Å; $\beta = 99.59$ (2)°; $V = 1590$ Å^3; $R = 0.049$ for 2285 reflections having $F_o^2 > 3\sigma(F_o^2)$. Crystal data for **3**: mol wt 619; space group $P2_1$; $Z = 2$; $a = 8.307$ (2), $b = 15.310$ (5), $c = 12.540$ (3) Å; $\beta = 99.72$ (2)°; $V = 1572$ Å^3; $R = 0.030$ for 3352 reflections having $F_o^2 > 3\sigma(F_o^2)$.

Introduction

Extensive studies of *closo*-MC_2B_4 metallacarborane clusters derived from the *nido*-$R_2C_2B_4H_4^{2-}$ ligand, where M is a transition or main-group metal, have been conducted in a number of laboratories,[2,3] facilitated by the ready availability of the *nido*-2,3-

(1) (a) Taken in part from: Boyter, H. A., Jr. M.S. Thesis University of Virginia, 1984. (b) Present address: PPG Fiber Glass Division, Pittsburgh, PA.

(2) Recent reviews: (a) Leach, J. B. *Organomet. Chem.* **1982**, *10*, 48. (b) Grimes, R. N. In "Comprehensive Organometallic Chemistry"; Wilkinson, G., Stone, F. G. A., Abel, E., Eds.; Pergamon Press: Oxford, England, 1982; Chapter 5.5. (c) Grimes, R. N. *Coord. Chem. Rev.* **1979**, *28*, 55.

0020-1669/85/1324-3810$01.50/0

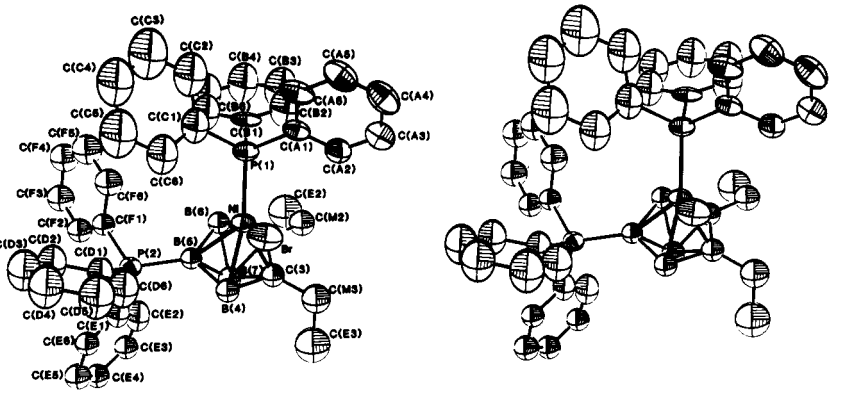

Figure 1. Stereoview of molecular structure of **1**.

Table I. 115.8-MHz ^{11}B FT NMR Data (CH_2Cl_2 Solution)

compd	δ (J, Hz)[a]	rel area
1,2,3-$(Ph_3P)(Br)Ni(Et_2C_2B_4H_3$-5-$PPh_3)$ (**1**)[b]	7.93, 8.54, 3.63, −0.76	2:2:3:3
1,2,3-$(Ph_2PCH_2)_2(Cl)Co(Et_2C_2B_4H_4)$ (**2**)	11.61 (110), 4.67, −0.35	1:2:1
1,2,3-$(Ph_2PCH_2)_2(CN)Co(Et_2C_2B_4H_4)$ (**4**)	15.83 (88), 7.16	1:3
1,2,3-$(Ph_2PCH_2)_2(I)Co(Et_2C_2B_4H_5)$ (**5**)	13.84, 5.80	1:3

[a] Vs. $BF_3{\cdot}OEt_2$; negative shifts upfield. Where B–H coupling is omitted, it was not measurable. [b] Spectrum indicates presence of more than one species in solution (see text).

$R_2C_2B_4H_6$ carborane precursor.[4] Except for the family of 12-vertex icosahedral MC_2B_9 systems,[2a,b,5] the 7-vertex MC_2B_4 and $M_2C_2B_3$ clusters form by far the largest structural class of metallacarboranes, and hundreds have been prepared and characterized. The majority of the known compounds contain a first-row transition metal with an attached η^5-C_5H_5 or arene ligand, and these groups are not, in general, readily displaceable. Hence the chemistry of the metal centers in the seven-vertex cages, including potential catalytic properties (well-known in larger metallacarboranes[6]), has scarcely been explored other than the oxidative fusion reaction[7] in $M(C_2B_4)_2$ complexes. In the present study we set out to develop synthetic routes to $L_nM(R_2C_2B_4H_4)$ species in which L is a phosphino or other σ-bonded ligand and to explore the reactivity of such complexes at the metal vertex. As it developed, however, the main isolated products contained halogen as well as phosphino ligands on the metal, in turn affecting the subsequent chemical investigations.

Scheme I

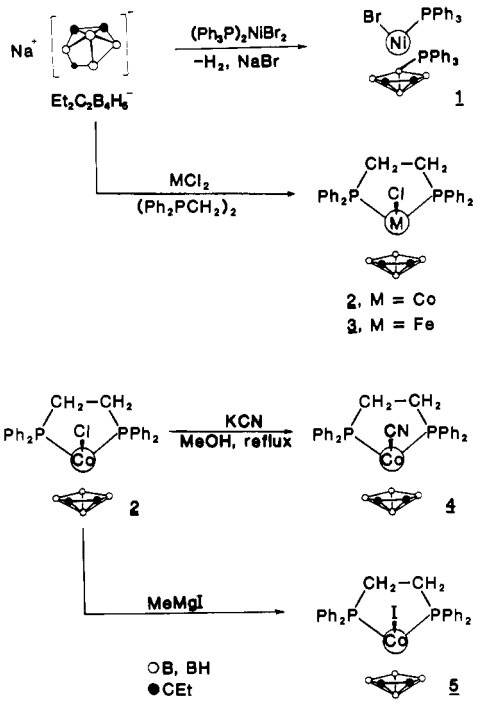

Table II. 360-MHz ^1H FT NMR Data

compd	δ	rel area	assignmt
2 (C_6D_6)	8.41 t, 7.62 t, 7.15 m, 6.98 t	5:5:5:5	C_6H_5
	2.66 m	4	diphos CH_2
	2.51 m	4	ethyl CH_2
	1.22 t	6	CH_3
2 (acetone-d_6)	8.31 t, 7.76 t, 7.60 m, 7.45 t	5:5:5:5	C_6H_5
	2.74 m	4	diphos CH_2
	2.30 m	4	ethyl CH_2
	1.08 t	6	CH_3
4 (acetone-d_6)	7.91 t, 7.67 t, 7.52 m, 7.39 t	5:4:6:5	C_6H_5
	2.46 m	4	diphos CH_2
	2.26 m	4	ethyl CH_2
	1.15 t	6	CH_3
5 ($CDCl_3$)	7.92 t, 7.54 t, 7.44 t, 7.26[b]	5:5:5:5[b]	C_6H_5
	2.516–2.630[c]	8	diphos CH_2, ethyl CH_2
	1.08 t	6	CH_3

[a] Legend: m = multiplet, d = doublet, t = triplet. [b] Estimated; multiplet partly overlapped with solvent peak. [c] Overlapping multiplets.

(3) (a) Hosmane, N. S.; Sirmokadam, N. N. *Organometallics*, **1984**, *3*, 1119. (b) Hosmane, N. S.; Sirmokadam, N. N.; Herber, R. H. *Ibid.* **1984**, *3*, 1665. (c) Micciche, R. P.; Sneddon, L. G. *Ibid.* **1983**, *2*, 674. (d) Micciche, R. P.; Brugiglio, J. J.; Sneddon, L. G. *Ibid.* **1984**, *3*, 1396. (e) Barker, G. K.; Green, M.; Stone, F. G. A.; Welch, A. J. *J. Chem. Soc., Dalton Trans.* **1980**, 1186. (f) Barker, G. K.; Garcia, M. P.; Green, M.; Stone, F. G. A.; Welch, A. J. *Ibid.* **1982**, 1679. (g) Grimes, R. N.; Rademaker, W. J.; Denniston, M. L.; Bryan, R. F.; Greene, P. T. *J. Am. Chem. Soc.* **1972**, *94*, 1865. Miller, V. R.; Grimes, R. N. *Ibid.* **1973**, *95*, 2830. (h) Miller, V. R.; Sneddon, L. G.; Beer, D. C.; Grimes, R. N. *Ibid.* **1974**, *96*, 3090. (i) Maxwell, W. M.; Miller, V. R.; Grimes, R. N. *Ibid.* **1976**, *98*, 4818. (j) Sneddon, L. G.; Beer, D. C.; Grimes, R. N. *Ibid.* **1973**, *95*, 6623. (k) Grimes, R. N.; Beer, D. C.; Sneddon, L. G.; Miller, V. R.; Weiss, R. *Inorg. Chem.* **1974**, *13*, 1138. (l) Maxwell, W. M.; Wong, K.-S.; Grimes, R. N. *Ibid.* **1977**, *16*, 3094. (m) Maxwell, W. M.; Miller, V. R.; Grimes, R. N. *Ibid.* **1976**, *15*, 1343. (n) Wong, K.-S.; Grimes, R. N. *Ibid.* **1977**, *16*, 2053. (o) Borodinsky, L.; Grimes, R. N. *Ibid.* **1982**, *21*, 1921. (p) Maynard, R. B.; Swisher, R. G.; Grimes, R. N. *Organometallics* **1983**, *2*, 500. (q) Swisher, R. G.; Sinn, E.; Grimes, R. N. *Ibid.* **1983**, *2*, 506. (r) Swisher, R. G.; Sinn, E.; Grimes, R. N. *Ibid.* **1984**, *3*, 599. (s) Swisher, R. G.; Butcher, R. J.; Sinn, E.; Grimes, R. N. *Ibid.* *4*, 882. (t) Swisher, R. G.; Sinn, E.; Grimes, R. N. *Ibid.* *4*, 890, 896.
(4) Maynard, R. B.; Borodinsky, L.; Grimes, R. N. *Inorg. Synth.* **1983**, *22*, 211.
(5) Dunks, G. B.; Hawthorne, M. F. In "Boron Hydride Chemistry"; Muetterties, E. L., Ed.; Academic Press: New York, 1975; Chapter 11.
(6) Behnken, P. E.; Busby, D. C.; Delaney, M. S.; King, R. E., III; Kreimendahl, C. W.; Marder, T. B.; Wilczynski, J. J.; Hawthorne, M. F. *J. Am. Chem. Soc.* **1984**, *106*, 7444 and references therein.
(7) Maynard, R. B.; Grimes, R. N. *J. Am. Chem. Soc.* **1982**, *104*, 5983 and references therein.

Table III. Infrared Absorptions (cm^{-1})

1[a] 3060 m, 2970 m, 2930 m, 2870 w, 2540 s, 1650 w, br, 1495 s, 1445 vs, 1390 w, 1350 vw, 1325 w, 1200 m, 1175 w, 1117 s, 1085 w, 1040 m, 1110 m, 960 vw, 880 w, 755 s, 703 vs, 630 w, 525 vs, 450 w, br

2[a] 3140 w, 3110 w, 3100 sh, 3020 m, 2985 m, 2920 w, 2620 s, 2590 s, 1615 w, 1605 w, 1345 w, 1220 w, 1120 s, 1100 w, 1055 w, 1030 w, 1010 sh, 985 w, 940 w, 900 s, 825 m, 770 s, 715 s, 695 s, 680 m, 550 s, 505 s, 465 w, 420 w, 375 w

3[a] 3150 w, 3120 w, 3110 sh, 3020 m, 2995 m, 2920 m, 264· s, 2595 s, 2590 s, 1765 m, 1520 m, 1465 s, 1440 w, 1320 w, ·.·0 w, 1125 s, 1100 w, 1060 w, 1030 w, 1020 w, 910 s, 835 m, 780 s, 720 s, 700 s, 555 s, 520 m

4[b] 3070 w, 2970 m, 2920 m, 2870 w, 2860 w, 2545 s, 2120 w, 2100 w, 1640 w, 1430 m, 1090 w, 1030 w, 950 m, 690 s, 525 m

5[b] 3070 sh, 3020 w, 2940 s, 2895 s, 2830 sh, 2820 m, 2520 s, 1475 m, 1420 s, 1225 w, 1080 m, 1015 m, 940 m, 680 s, 520 s

[a] KBr pellet. [b] CCl_4 solution vs. CCl_4.

Results and Discussion

Reaction of $Na^+Et_2C_2B_4H_5^-$ with $(Ph_3P)_2NiBr_2$. Some time ago the seven-vertex closo species 1,2,4-$(Ph_3P)_2NiC_2B_4H_6$ was obtained[3h] in our laboratory via direct metal insertion in the reaction of $(C_2H_4)Ni(Ph_3P)_2$ with *closo*-1,6-$C_2B_4H_6$, a stable but relatively inaccessible carborane. In the present study, the preparation of the analogous complex 1,2,3-$(Ph_3P)_2Ni(Et_2C_2B_4H_4)$ was attempted via treatment of the 2,3-$Et_2C_2B_4H_5^-$ ion with dibromobis(triphenylphosphino)nickel(II) in THF. The expected compound was not found; instead; the main isolated product was 1-Br-1,5-$(Ph_3P)_2$-1,2,3-$Ni(Et_2C_2B_4H_3)$ (**1**) as depicted in Scheme I. This metallacarborane was obtained in 27% yield as a purple, moderately air-sensitive solid and characterized from its ^{11}B NMR (Table I), IR (Table III), UV–visible, and mass spectra and from X-ray diffraction data. As shown in Scheme I and in an ORTEP view of the molecule (Figure 1), one of the phosphine ligands has been displaced from the metal by a bromine atom and is attached at a boron vertex, B(5). The formula of **1** indicates net loss of H_2 and NaBr from the starting reagents (Scheme I), although only **1** was identified from the product mixture.

The electron-impact (EI) mass spectrum of **1** exhibits a weak parent group between *m/e* 797 and 787 with a base peak at *m/e* 792, which corresponds to the pattern calculated for this composition from natural isotope abundances. The 115.8-MHz ^{11}B FT NMR spectrum reveals at least four distinguishable BH environments, but the pattern is more complex than would be anticipated for **1** alone; hence we believe **1** may be in equilibrium in solution with a dimer (possibly linked via two Ni–Br–Ni bridges). The solid-state structure of **1** was, however, unequivocally established by X-ray crystallography as described below.

The triphenylphosphine migration observed in the formation of **1** has precedent (at least in net effect, if not in actual mechanism) in the conversion of the 12-vertex *closo*-metallacarborane 1,2,3-$(Ph_3P)_2NiC_2B_9H_{11}$ to the hydrido complex *closo*-(Ph_3P)-$(H)NiC_2B_9H_{10}$-8-PPh_3 in refluxing benzene at 80 °C; treatment of this compound with HCl gas displaces the H^- ligand and generates the corresponding metal–chloro species, *closo*-$(Ph_3P)(Cl)NiC_2B_9H_{10}$-8-$PPh_3$.[8] This compound is structurally related to **1**, with the B–PPh_3 group in both cases located on the bonding face to the metal and nonadjacent to carbon. Phosphine migrations from metal to boron vertices have also been observed in the thermolysis of *nido*-9,7,8-$(Et_3P)_2HPtC_2B_8H_{11}$ to 9,7,8-$(Et_3P)(H)PtC_2B_8H_9$-10-PEt_3 at 100 °C[9] and in the reaction of the $CB_8H_{13}^-$ ion with $Ir(Cl)(PPh_3)_3$ over 6 days in ether at 20 °C,[10] which yields a closo 10-vertex species, 2,10-$(Ph_3P)_2(H)$-$IrCB_8H_8$-1-PPh_3. In all these cases, the proposed mechanisms involve dissociation of phosphine from the metal at some stage followed by attack of the phosphine at a boron vertex. In our work, a similar dissociative process undoubtedly leads to the formation of **1**, but the reaction in this case appears more facile than in most previous examples in that it occurs at room temperature with no detectable intermediate complex.

Table IV. Experimental Parameters and Crystal Data

	1	**2**	**3**
mol wt	792	622	619
space group	$P\bar{1}$	$P2_1$	$P2_1$
a, Å	11.115 (4)	8.311 (2)	8.307 (2)
b, Å	12.497 (5)	15.357 (3)	15.310 (5)
c, Å	14.358 (8)	12.635 (5)	12.540 (3)
α, deg	90.34 (4)		
β, deg	94.57 (4)	99.59	99.72 (2)
γ, deg	91.80 (2)		
V, $Å^3$	1987	1590	1572
μ, cm^{-1}	16.6	7.8	7.0
D(calcd), g/cm^3	1.32	1.32	1.31
A[a]	0.60	0.60	0.60
B[a]	0.35	0.35	0.35
max trans coeff	0.613	0.939	0.873
min trans coeff	0.551	0.914	0.690
2θ range, deg	1–56	2.4–54	2–54
no. of reflctns obsd	5849	3233	4095
no. of reflctns refined	4741	2285	3352
R	0.059	0.049	0.030
R_w	0.070	0.056	0.037
esd unit wt	3.0	1.5	0.82
Z	2.0	2	2
cryst dimens	100 (0.28)	100 (0.08)	100 (0.049)
(cm from centroid)	$\bar{1}00$ (0.28)	$\bar{1}00$ (0.08)	$\bar{1}00$ (0.049)
	011 (0.30)	010 (0.028)	$1\bar{1}0$ (0.035)
	$0\bar{1}\bar{1}$ (0.30)	$0\bar{1}0$ (0.028)	011 (0.028)
	$0\bar{1}1$ (0.40)	001 (0.05)	$0\bar{1}\bar{1}$ (0.028)
	$01\bar{1}$ (0.40)	$00\bar{1}$ (0.05)	$01\bar{1}$ (0.033)
			$0\bar{1}1$ (0.033)
			001 (0.015)
			$00\bar{1}$ (0.015)

[a] For explanation, see Experimental Section.

X-ray Structure Determination on 1. The data collection parameters and information on the crystal are given in Table IV, while Tables V–VII list atomic coordinates, interatomic distances, and bond angles. The NiC_2B_4 cage has regular closo geometry, as expected for a 7-vertex 16-skeletal-electron system,[11] and the framework bond lengths are closely comparable to those of other MC_2B_4 clusters. However, despite many published X-ray structure determinations on MC_2B_4 systems of iron,[3c,f,p,q,s,t,12] cobalt,[3f,12a,13] and other metals,[3e,g,r] prior to this work there were none involving nickel. Indeed, only two NiC_2B_4 cage compounds—1,2,4-$(Ph_3P)_2NiC_2B_4H_6$ (mentioned above) and 1,2,3-$(Ph_2PCH_2)_2NiC_2B_4H_6$[3k]—have been prepared.

The Ni-Br bond length of 2.33 Å is as expected from the sum of covalent radii; comparisons with similar species are not possible since no other bonded M–X distances in metal–boron clusters, where M is a first-row transition metal and X is a halogen, are available. (Structures of several metallacarboranes containing Rh–Cl or Rh–Br bonds have been reported, however.[14])

(8) King, R. E., III; Miller, S. B.; Knobler, C. B.; Hawthorne, M. F. *Inorg. Chem.* **1983**, *22*, 3548.
(9) Barker, G. K.; Green, M.; Stone, F. G. A.; Wosley, W. C.; Welch, A. J. *J. Chem. Soc., Dalton Trans.* **1983**, 2063.
(10) Alcock, N. W.; Taylor, J. G.; Wallbridge, M. G. H. *J. Chem. Soc., Chem. Commun.* **1983**, 1168.
(11) (a) O'Neill, M. E.; Wade, K. In "Metal Interactions with Boron Clusters"; Grimes, R. N.; Ed.; Plenum Press: New York, 1982; Chapter 1 and references therein. (b) Mingos, D. M. P. *Acc. Chem. Res.* **1984**, *17*, 311.
(12) (a) Maxwell, W. M.; Sinn, E.; Grimes, R. N. *J. Am. Chem. Soc.* **1976**, *98*, 3490. (b) Pipal, J. R.; Grimes, R. N. *Inorg. Chem.* **1979**, *18*, 263. (c) Grimes, R. N.; Maynard, R. B.; Sinn, E.; Brewer, G. A.; Long, G. J. *J. Am. Chem. Soc.* **1982**, *104*, 5987.
(13) (a) Weiss, R.; Bryan, R. F. *Acta Crystallogr., Sect. B: Struct. Crystallogr. Cryst. Chem.* **1977**, *B33*, 589. (b) Borelli, A. J. Jr.; Plotkin, J. S.; Sneddon, L. G. *Inorg. Chem.* **1982**, *21*, 1328. (c) Pipal, J. R.; Maxwell, W. M.; Grimes, R. N. *Ibid.* **1978**, *17*, 1447. (d) Borodinsky, L.; Sinn, E.; Grimes, R. N. *Ibid.* **1982**, *21*, 1928.
(14) (a) Zheng, L.; Baker, R. T.; Knobler, C. B.; Walker, J. A.; Hawthorne, M. F. *Inorg. Chem.* **1983**, *22*, 3350. (b) Baker, R. T.; Delaney, M. S.; King, R. E., III; Knobler, C. B.; Long, J. A.; Marder, T. B.; Paxson, T. E.; Teller, R. E.; Hawthorne, M. F. *J. Am. Chem. Soc.* **1984**, *106*, 2965.

Table V. Positional Parameters and Their Estimated Standard Deviations for 1-Br-1,5-$(Ph_3P)_2$-1,2,3-Ni($Et_2C_2B_4H_3$) (**1**)

atom	x	y	z	atom	x	y	z
Br	0.1906 (1)	−0.02418 (7)	0.26577 (7)	C(3)	0.1463 (7)	−0.2219 (7)	0.0951 (5)
Ni	0.23660 (9)	−0.19945 (7)	0.23035 (6)	C(3M)	0.0297 (8)	−0.1836 (9)	0.0497 (7)
P(1)	0.2354 (2)	−0.2488 (1)	0.3749 (1)	C(3E)	0.0277 (12)	−0.1635 (13)	−0.0530 (8)
P(2)	0.5422 (2)	−0.2402 (2)	0.1184 (1)	B(4)	0.2734 (8)	−0.1611 (8)	0.0910 (6)
C(A1)	0.1088 (7)	−0.1999 (5)	0.4324 (5)	B(5)	0.3751 (8)	−0.2429 (7)	0.1329 (5)
C(A2)	−0.0052 (8)	−0.2059 (7)	0.3859 (5)	B(6)	0.2972 (8)	−0.3414 (7)	0.1767 (6)
C(A3)	−0.1054 (8)	−0.1727 (8)	0.4253 (6)	B(7)	0.2620 (8)	−0.3005 (8)	0.0588 (6)
C(A4)	−0.0955 (8)	−0.1298 (7)	0.5149 (6)	H(A2)	−0.010 (7)	−0.233 (6)	0.333 (5)
C(A5)	0.0157 (9)	−0.1227 (7)	0.5604 (6)	H(A3)	−0.182 (7)	−0.179 (6)	0.396 (5)
C(A6)	0.1158 (8)	−0.1564 (7)	0.5225 (5)	H(B2)	0.047 (6)	−0.412 (5)	0.408 (4)
C(B1)	0.2301 (8)	−0.3936 (6)	0.3983 (5)	H(B3)	0.051 (7)	−0.592 (6)	0.423 (5)
C(B2)	0.1232 (9)	−0.4493 (7)	0.4073 (6)	H(B4)	0.233 (6)	−0.682 (6)	0.424 (5)
C(B3)	0.1267 (11)	−0.5611 (8)	0.4183 (7)	H(B5)	0.411 (6)	−0.595 (6)	0.411 (5)
C(B4)	0.2302 (12)	−0.6116 (7)	0.4185 (6)	H(B6)	0.408 (6)	−0.413 (6)	0.396 (5)
C(B5)	0.3361 (10)	−0.5579 (7)	0.4109 (6)	H(C2)	0.328 (7)	−0.284 (6)	0.562 (5)
C(B6)	0.3359 (9)	−0.4484 (6)	0.4013 (5)	H(C3)	0.502 (7)	−0.226 (6)	0.651 (5)
C(C1)	0.3709 (7)	−0.2060 (6)	0.4466 (5)	H(C4)	0.642 (7)	−0.124 (6)	0.585 (6)
C(C2)	0.3898 (9)	−0.2392 (8)	0.5392 (6)	H(C5)	0.618 (7)	−0.063 (6)	0.435 (5)
C(C3)	0.4912 (10)	−0.2032 (9)	0.5916 (7)	H(C6)	0.449 (7)	−0.119 (6)	0.344 (5)
C(C4)	0.5736 (9)	−0.1389 (9)	0.5558 (7)	H(D2)	0.791 (6)	−0.173 (5)	0.184 (4)
C(C5)	0.5592 (9)	−0.1064 (8)	0.4650 (8)	H(D3)	0.890 (6)	−0.016 (6)	0.226 (5)
C(C6)	0.4550 (8)	−0.1407 (7)	0.4102 (6)	H(D4)	0.771 (7)	0.137 (6)	0.226 (5)
C(D1)	0.6164 (7)	−0.1156 (6)	0.1602 (5)	H(D5)	0.568 (6)	0.133 (6)	0.189 (5)
C(D2)	0.7402 (8)	−0.1137 (7)	0.1861 (6)	H(D6)	0.468 (6)	−0.028 (5)	0.152 (5)
C(D3)	0.7982 (8)	−0.0165 (7)	0.2137 (6)	H(E2)	0.473 (6)	−0.389 (5)	−0.024 (5)
C(D4)	0.7333 (9)	0.0733 (7)	0.2142 (6)	H(E3)	0.534 (7)	−0.428 (6)	−0.171 (5)
C(D5)	0.6119 (9)	0.0724 (7)	0.1885 (7)	H(E4)	0.669 (7)	−0.315 (6)	−0.231 (5)
C(D6)	0.5537 (8)	−0.0246 (7)	0.1618 (6)	H(E5)	0.743 (6)	−0.168 (6)	−0.156 (5)
C(E1)	0.5787 (6)	−0.2562 (6)	−0.0012 (4)	H(E6)	0.692 (6)	−0.130 (5)	−0.012 (5)
C(E2)	0.5292 (8)	−0.3449 (6)	−0.0514 (5)	H(F2)	0.707 (6)	−0.410 (6)	0.084 (5)
C(E3)	0.5620 (8)	−0.3649 (7)	−0.1402 (5)	H(F3)	0.808 (6)	−0.538 (6)	0.166 (5)
C(E4)	0.6423 (8)	−0.2989 (8)	−0.1786 (5)	H(F4)	0.782 (6)	−0.551 (6)	0.321 (5)
C(E5)	0.6890 (8)	−0.2105 (8)	−0.1326 (5)	H(F5)	0.655 (7)	−0.430 (6)	0.385 (5)
C(E6)	0.6590 (7)	−0.1895 (6)	−0.0418 (5)	H(F6)	0.553 (6)	−0.306 (6)	0.303 (5)
C(F1)	0.6219 (6)	−0.3457 (6)	0.1814 (5)	H(21M)	−0.007 (6)	−0.390 (6)	0.101 (5)
C(F2)	0.6943 (7)	−0.4163 (7)	0.1431 (5)	H(22M)	0.021 (6)	−0.399 (6)	0.202 (5)
C(F3)	0.7528 (8)	−0.4937 (8)	0.1942 (7)	H(31M)	0.007 (6)	−0.117 (6)	0.076 (5)
C(F4)	0.7407 (9)	−0.5000 (9)	0.2881 (7)	H(32M)	−0.036 (6)	−0.231 (6)	0.064 (5)
C(F5)	0.6695 (10)	−0.4317 (9)	0.3274 (6)	H(4)	0.286 (6)	−0.096 (5)	0.045 (4)
C(F6)	0.6081 (9)	−0.3544 (8)	0.2778 (6)	H(6)	0.318 (6)	−0.408 (5)	0.205 (4)
C(2)	0.1603 (7)	−0.3237 (6)	0.1420 (5)	H(7)	0.262 (6)	−0.355 (5)	−0.000 (4)
C(2M)	0.0578 (8)	−0.4073 (8)	0.1469 (6)				
C(2E)	0.0933 (12)	−0.5183 (8)	0.1317 (11)				

The triphenylphosphine ligands are well defined, all phenyl rings being planar within experimental error. Despite their attachment at nickel and boron vertices, respectively, the PPh_3 groups are almost identical, each displaying small internal C–C–C angles at C(1) (the point of attachment at phosphorus) and relatively long C–C bonds in the vicinity of C(1); both effects suggest larger p character (hybridization between sp^2 and sp^3) on C(1) compared to other ring carbons. The nickel–phosphorus distance in **1** is significantly shorter (by 0.02–0.08 Å) than the corresponding bonds in *nido*-$(Ph_2PCH_2)_2NiMe_4C_4B_8H_8$ [2.194 (1) Å][15] and *arachno*-$(Et_3P)_2NiMe_2C_2B_7H_9$ [2.252 (2) and 2.213 (2) Å],[16] and the boron–phosphorus length in **1** is 0.03–0.05 Å less than the B–P distances in $(Et_3P)(H)PtC_2B_7H_9$-10-PEt_3[9] and $(\mu\text{-}CO)_2(NiC_2B_9H_{10}\text{-}8\text{-}PPh_3)_2$.[8] The P(1)–Ni–Br angle close to 90° is consistent with square-planar hybridization on nickel, whose linkage to the carborane face would then be mainly via B(4) and B(6) with weaker bonding to the other three atoms; inspection of the bond lengths involved lends some support to this idea, although the Ni–C distances imply significant metal–carbon interactions as well. A square-planar configuration for nickel would be consistent with its formal +2 oxidation state in this complex.

Reactions of $Na^+Et_2C_2B_4H_5^-$ with $(Ph_2PCH_2)_2$ and $FeCl_2$ or $CoCl_2$. In an alternative approach to the synthesis of small phosphinometallacarboranes, the readily accessible ligand 1,2-bis(diphenylphosphino)ethane, "diphos", was employed in reactions with metal halides and the carborane anion. The order of addition of reagents is crucial, since the reaction of $CoCl_2$ with carborane anion followed by diphos yields only the ethyl homologue of the known[3i] bis(carboranyl) complex $HCo(Me_2C_2B_4H_4)_2$. However, if the diphos is present at the start, the reaction proceeds as shown in Scheme I. (Compound **3** is also formed in low yield in the reaction of $H_2Fe(Et_2C_2B_4H_4)_2$ with diphos and $CoCl_2$.) The metallacarborane products were characterized as $(Ph_2PCH_2)_2(Cl)M(Et_2C_2B_4H_4)$ (**2**, M = Co; **3**, M = Fe), the metal having a formal oxidation state of +3 in each case. Both complexes exhibit EI mass spectra whose parent peak envelopes are consistent with the calculated patterns based on natural isotope abundances, as well as fragments corresponding to the loss of chlorine and of the carborane ligand from the parent ion. The cobalt species **2** was further characterized from its ^{11}B, ^1H, and ^{31}P FT NMR, IR, and UV–visible spectra (see Experimental Section). The iron complex **3** is paramagnetic, and NMR spectra were not observable; however, the structures of **2** and **3** (Figure 2) were established via X-ray diffraction studies, described below.

The 360-MHz NMR spectrum of **2**, shown in Figure 3, displays unusually well-resolved phenyl resonances for which there is little precedent in the literature. In most metal–diphos complexes, the phenyl region appears as a single peak or a broad multiplet;[3k,17]

(15) Grimes, R. N.; Sinn, E.; Pipal, J. R. *Inorg. Chem.* **1980**, *19*, 2087.
(16) Green, M.; Howard, J. A. K.; Spencer, J. L.; Stone, F. G. A. *J. Chem. Soc., Dalton Trans.* **1975**, 2274.
(17) (a) Felkin, H.; Knowles, P. J.; Meunier, B.; Mitschler, A.; Ricard, L.; Weiss, R. *J. Chem. Soc., Chem. Commun.* **1974**, *44*. (b) Maxwell, W. M.; Bryan, R. F.; Grimes, R. N. *J. Am. Chem. Soc.* **1977**, *99*, 4008. (c) Kaempfe, L. A.; Barnett, K. W. *Inorg. Chem.* **1973**, *12*, 2578. (d) Frizzell, J. J.; Luck, R. L.; Morris, R. H.; Peng, S. H. *J. Organomet. Chem.* **1985**, *284*, 243.

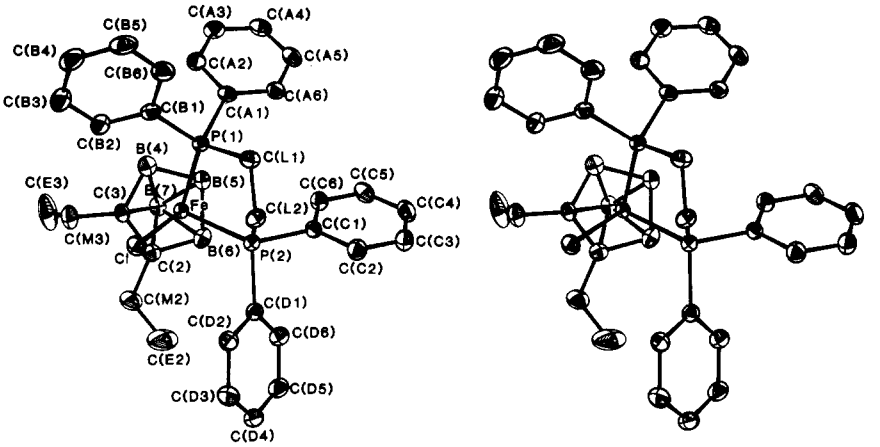

Figure 2. Stereoview of molecular structure of **3** (isostructural with **2**). Atom labels are identical in **2** and **3**.

Table VI. Bond Distances (Å) in **1**

Ni-Br	2.327 (1)	C(D1)-C(D6)	1.353 (5)
Ni-P(1)	2.170 (1)	C(D2)-C(D3)	1.398 (5)
Ni-C(2)	2.113 (3)	C(D3)-C(D4)	1.353 (5)
Ni-C(3)	2.127 (3)	C(D4)-C(D5)	1.370 (6)
Ni-B(4)	2.128 (3)	C(D5)-C(D6)	1.393 (5)
Ni-B(5)	2.238 (3)	C(E1)-C(E2)	1.394 (4)
Ni-B(6)	2.082 (3)	C(E1)-C(E6)	1.369 (4)
P(1)-C(A1)	1.808 (3)	C(E2)-C(E3)	1.377 (4)
P(1)-C(B1)	1.843 (3)	C(E3)-C(E4)	1.348 (5)
P(1)-C(C1)	1.819 (3)	C(E4)-C(E5)	1.352 (5)
P(2)-C(D1)	1.816 (3)	C(E5)-C(E6)	1.396 (5)
P(2)-C(E1)	1.806 (3)	C(F1)-C(F2)	1.356 (4)
P(2)-C(F1)	1.816 (3)	C(F1)-C(F6)	1.409 (4)
P(2)-B(5)	1.884 (4)	C(F2)-C(F3)	1.368 (5)
C(A1)-C(A2)	1.384 (4)	C(F3)-C(F4)	1.368 (6)
C(A1)-C(A6)	1.396 (4)	C(F4)-C(F5)	1.335 (6)
C(A2)-C(A3)	1.362 (5)	C(F5)-C(F6)	1.370 (5)
C(A3)-C(A4)	1.386 (5)	C(2)-C(2M)	1.527 (5)
C(A4)-C(A5)	1.352 (5)	C(2)-C(3)	1.450 (5)
C(A5)-C(A6)	1.354 (5)	C(2)-B(6)	1.586 (5)
C(B1)-C(B2)	1.373 (5)	C(2)-B(7)	1.729 (5)
C(B1)-C(B6)	1.377 (5)	C(2M)-C(2E)	1.473 (6)
C(B2)-C(B3)	1.408 (5)	C(3)-C(3M)	1.497 (5)
C(B3)-C(B4)	1.330 (7)	C(3)-B(4)	1.588 (5)
C(B4)-C(B5)	1.348 (7)	C(3)-B(7)	1.752 (5)
C(B5)-C(B6)	1.376 (5)	C(3M)-C(3E)	1.496 (6)
C(C1)-C(C2)	1.397 (5)	B(4)-B(5)	1.630 (5)
C(C1)-C(C6)	1.358 (5)	B(4)-B(7)	1.798 (6)
C(C2)-C(C3)	1.366 (6)	B(5)-B(6)	1.640 (5)
C(C3)-C(C4)	1.336 (8)	B(5)-B(7)	1.719 (5)
C(C4)-C(C5)	1.366 (7)	B(6)-B(7)	1.788 (5)
C(C5)-C(C6)	1.402 (5)	⟨B-H⟩	1.035
C(D1)-C(D2)	1.395 (4)	⟨C-H⟩	0.924

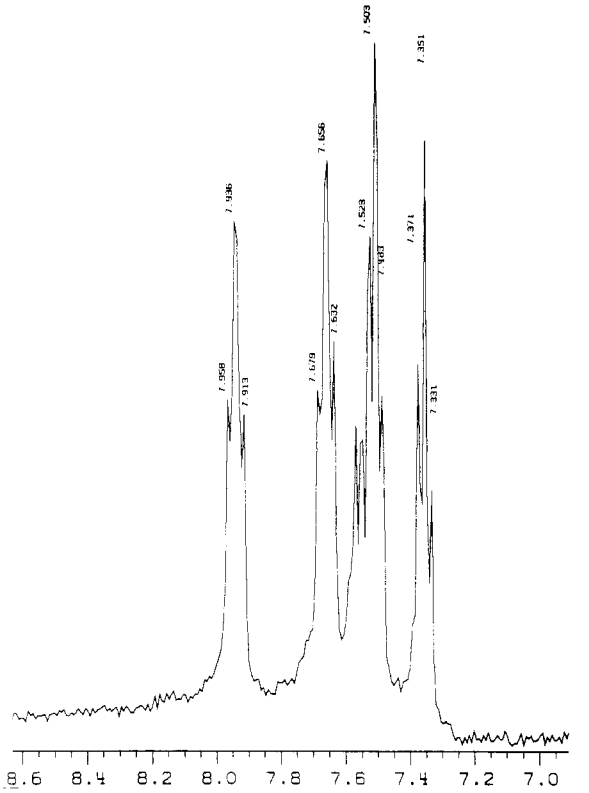

Figure 3. Phenyl region of 360-MHz ^{1}H FT NMR spectrum of **2** in $(CD_3)_2CO$.

recently, however, the 200-MHz ^{1}H spectrum of (diphos)Mo(η^6-PhPPh$_2$)(CN-*t*-Bu) has been shown to exhibit exceptional resolution of the diphos phenyl resonances similar to that observed in **3**.[17d] This effect may be associated with the η^6-arene ligand on the metal, and it is reasonable to infer that the carborane ligand in **3** similarly influences the diphos proton shifts in that species. In **3**, the ^{31}P NMR spectrum contains a single resonance, showing that inequivalence in the two phosphorus environments is not detectable on the NMR time scale.

The UV-visible spectra of **2** and **3** exhibit peaks near 260 and 460 nm, which are assigned to the phenyl rings and metal d-d transitions, respectively.[18] The paramagnetism of **3**, a formal 17-electron Fe(III) complex, was investigated via magnetic and ESR measurements. The effective magnetic moment of 1.92 μ_B is consistent with a low-spin d^5 configuration, as are the ESR spectra of solid and CH_2Cl_2 solution samples, which at room temperature gave one-line spectra with g = 2.05 and 2.106, respectively; at 77 K, the solution spectrum gave g = 2.065. The essential identity of the cage geometry in **2** and **3** (vide infra) suggests that the unpaired electron in the iron complex resides in a nonbonding metal orbital and does not significantly affect the cluster bonding.

Reactions of $(Ph_2PCH_2)_2(Cl)Co(Et_2C_2B_4H_4)$ (2). In contrast to analogous cyclopentadienyliron complexes,[19] neither **2** nor **3** undergoes exchange of the halogen ligand for H$^-$, both metallacarboranes being unreactive toward NaH in THF and unstable toward $LiAlH_4$, at room temperature. However, it was possible to effect replacement of the chloride in **2** with cyanide via treatment with KCN in refluxing methanol (Scheme I). The main product **4**, a green-yellow oil, was characterized from its mass spectrum, which exhibits a parent grouping at m/e 615 closely matching the calculated intensities, and its ^{11}B, ^{1}H, and ^{31}P NMR,

(18) (a) Lambert, J. B.; Shurvill, H. F.; Verbit, L.; Cooks, R. G.; Stout, G. H. "Organic Structural Analysis"; Macmillan: New York, 1976; p 363. (b) Purcell, K. F.; Kotz, J. C., "Inorganic Chemistry"; W. B. Saunders: Philadelphia, 1977; pp 560-577.

(19) (a) Mays, M. J.; Sears, P. L. *J. Chem. Soc., Dalton Trans.* **1973**, 1873. (b) Treichel, P. M.; Molzahn, D. C. *Synth. React. Inorg. Met.-Org. Chem.* **1979**, *9*, 21. Davies, S. G.; Scott, F. *J. Organomet. Chem.* **1980**, *188*, C41.

Table VII. Selected Bond Angles (deg) in **1**

Br–Ni–P(1)	92.70 (8)	P(2)–C(D1)–C(D6)	120.3 (3)
Br–Ni–C(2)	136.66 (10)	C(D2)–C(D1)–C(D6)	120.4 (3)
Br–Ni–C(3)	102.10 (10)	C(D1)–C(D2)–C(D3)	119.0 (3)
Br–Ni–B(4)	93.12 (10)	C(D2)–C(D3)–C(D4)	119.3 (4)
Br–Ni–B(5)	123.86 (10)	C(D3)–C(D4)–C(D5)	122.2 (4)
Br–Ni–B(6)	167.97 (10)	C(D4)–C(D5)–C(D6)	118.6 (4)
P(1)–Ni–C(2)	109.49 (9)	C(D1)–C(D6)–C(D5)	120.5 (4)
P(1)–Ni–C(3)	143.41 (10)	P(2)–C(E1)–C(E2)	118.0 (2)
P(1)–Ni–B(4)	168.72 (1)	P(2)–C(E1)–C(E6)	122.9 (2)
P(1)–Ni–B(5)	125.40 (9)	C(E2)–C(E1)–C(E6)	118.9 (3)
P(1)–Ni–B(6)	97.58 (10)	C(E1)–C(E2)–C(E3)	120.0 (3)
Ni–P(1)–C(A1)	113.35 (10)	C(E2)–C(E3)–C(E4)	120.1 (3)
Ni–P(1)–C(B1)	117.48 (9)	C(E3)–C(E4)–C(E5)	121.1 (3)
Ni–P(1)–C(C1)	113.36 (12)	C(E4)–C(E5)–C(E6)	119.8 (3)
C(A1)–P(1)–C(B1)	103.46 (14)	C(E1)–C(E6)–C(E5)	119.9 (3)
C(A1)–P(1)–C(C1)	106.60 (14)	P(2)–C(F1)–C(F2)	125.2 (2)
C(B1)–P(1)–C(C1)	101.22 (15)	P(2)–C(F1)–C(F6)	117.5 (3)
C(D1)–P(2)–C(E1)	106.09 (13)	C(F2)–C(F1)–C(F6)	117.3 (3)
C(D1)–P(2)–C(F1)	105.74 (14)	C(F1)–C(F2)–C(F3)	122.6 (3)
C(D1)–P(2)–B(5)	112.23 (15)	C(F2)–C(F3)–C(F4)	119.5 (4)
C(E1)–P(2)–C(F1)	104.62 (14)	C(F3)–C(F4)–C(F5)	119.0 (4)
C(E1)–P(2)–B(5)	113.86 (14)	C(F4)–C(F5)–C(F6)	122.8 (4)
C(F1)–P(2)–B(5)	113.55 (15)	C(F1)–C(F6)–C(F5)	118.7 (4)
P(1)–C(A1)–C(A2)	119.2 (2)	Ni–C(2)–C(2M)	135.4 (2)
P(1)–C(A1)–C(A6)	124.9 (3)	Ni–C(2)–B(7)	93.1 (2)
C(A2)–C(A1)–C(A6)	115.8 (3)	C(2M)–C(2)–C(3)	123.6 (3)
C(A1)–C(A2)–C(A3)	122.6 (3)	C(2M)–C(2)–B(6)	124.9 (3)
C(A2)–C(A3)–C(A4)	120.2 (4)	C(2M)–C(2)–B(7)	131.5 (3)
C(A3)–C(A4)–C(A5)	117.6 (3)	C(3)–C(2)–B(6)	111.2 (3)
C(A4)–C(A5)–C(A6)	122.9 (3)	C(2)–C(2M)–C(2E)	114.3 (4)
C(A1)–C(A6)–C(A5)	120.9 (3)	Ni–C(3)–C(3M)	133.4 (3)
P(1)–C(B1)–C(B2)	122.0 (3)	Ni–C(3)–B(7)	91.9 (2)
P(1)–C(B1)–C(B6)	118.7 (3)	C(2)–C(3)–C(3M)	124.6 (3)
C(B2)–C(B1)–C(B6)	119.2 (3)	C(2)–C(3)–B(4)	110.7 (3)
C(B1)–C(B2)–C(B3)	118.1 (4)	C(3M)–C(3)–B(4)	124.6 (3)
C(B2)–C(B3)–C(B4)	121.0 (5)	C(3M)–C(3)–B(7)	134.7 (3)
C(B3)–C(B4)–C(B5)	121.6 (4)	C(3)–C(3M)–C(3E)	115.7 (4)
C(B4)–C(B5)–C(B6)	118.8 (4)	Ni–B(4)–B(7)	90.6 (2)
C(B1)–C(B6)–C(B5)	121.3 (4)	C(3)–B(4)–B(5)	106.5 (3)
P(1)–C(C1)–C(C2)	120.7 (3)	Ni–B(5)–P(2)	143.6 (2)
P(1)–C(C1)–C(C6)	119.9 (3)	P(2)–B(5)–B(4)	128.8 (2)
C(C2)–C(C1)–C(C6)	119.3 (3)	P(2)–B(5)–B(6)	126.0 (2)
C(C1)–C(C2)–C(C3)	119.1 (5)	P(2)–B(5)–B(7)	127.2 (3)
C(C2)–C(C3)–C(C4)	121.6 (5)	B(4)–B(5)–B(6)	104.4 (0)
C(C3)–C(C4)–C(C5)	121.0 (5)	Ni–B(6)–B(7)	92.4 (0)
C(C4)–C(C5)–C(C6)	118.6 (5)	C(2)–B(6)–B(5)	106.0 (0)
C(C1)–C(C6)–C(C5)	120.4 (4)	Ni–B(5)–B(7)	89.1 (2)
P(2)–C(D1)–C(D2)	119.1 (2)		

electronic, and IR spectra, which support a structure analogous to that of **2**. It is notable in the UV–visible spectrum of **4** that the band arising from metal d–d transitions occurs at 362 nm compared with 460 nm in **2**; this is consistent with attachment of the CN ligand in **4** to the metal rather than to the carborane cage. The IR spectrum of **4**, as expected, resembles those of **2** and **3** but contains a resonance at 2100 cm^{-1} assigned to the C≡N group.[17c,20]

Treatment of **2** with the Grignard reagent CH_3MgI was expected to produce $(Ph_2PCH_2)_2(CH_3)Co(Et_2C_2B_4H_4)$ by analogy with the synthesis of $(\eta^5\text{-}C_5H_5)M(CH_3)$ (M = Fe, Ru) from $(\eta^5\text{-}C_5H_5)M(L)$ (L = Cl, NCMe).[19] Instead, the only metallacarborane product isolated was an iodo derivative, $(Ph_2PCH_2)_2(I)Co(Et_2C_2B_4H_4)$ (**5**). While the reaction pathway leading to **5** is not known, a simple attack by I^- can be excluded since neither **2** nor **3** reacts with NaI in methanol at room temperature. The mass spectrum of **5** contains an intense parent envelope closely matching the calculated intensities and also exhibits fragments at *m/e* 586, 429, and 183, which correspond respectively to loss of I from the parent ion and to fragmentations of the (diphos)Co moiety. The ^{11}B, ^1H, and ^{31}P NMR spectra, and the UV–visible and IR spectra, are similar to those of **2** and support the proposed structure (Scheme I).

X-ray Structure Determinations on 2 and 3. As noted earlier, the cobalt and iron complexes **2** and **3** are isostructural, and they are essentially isomorphous as well. Tables IV and VIII–X present data collection and crystal parameters, atomic coordinates, and bond distances and angles, and an ORTEP view of complex **3** is given in Figure 2. Both molecules consist of closo (pentagonal bipyramidal) MC_2B_4 cages with exopolyhedral diphos and chloride ligands on the metal. However, since the paramagnetic iron(III) species **3** has one less electron than the diamagnetic cobalt complex **2**, it is of interest to look for significant structural differences. Insofar as the polyhedral cage is concerned, the two species are almost identical save for slightly shorter (by 0.04–0.08 Å) metal–carbon distances in **2**, which might partially reflect the smaller covalent radius of cobalt. There is certainly no perturbation of the closo geometry of **3** toward a hyper-closo (capped octahedral) shape,[21] which might have been expected if **3** had fewer than $2n + 2$ skeletal bonding electrons.[11] The two molecules do differ, however, in the metal–chlorine bond, the Fe–Cl distance being 0.022 Å (>10 standard deviations) shorter than the Co–Cl bond. Since this effect is in the opposite direction from that expected on the basis of covalent radii, we are inclined to associate the shorter Fe–Cl bond with the presence of only 17 electrons on iron. Thus, back-donation of electron density from chlorine to the electron-poor metal could account for the observed bond short-

(20) Ashby, G. S.; Bruce, M. I.; Tomkins, I. B.; Wallis, R. C. *Aust. J. Chem.* **1979**, *32*, 1003.

(21) Grimes, R. N. *Acc. Chem. Res.* **1983**, *16*, 22 and references therein.

Table VIII. Positional Parameters and Their Estimated Standard Deviations for **2** and **3**

2				**3**			
atom	*x*	*y*	*z*	atom	*x*	*y*	*z*
Co	0.1746 (1)	0.2500 (0)	0.23170 (8)	Fe	0.16638 (6)	0.2500 (0)	0.22625 (4)
Cl	0.3415 (3)	0.3182 (2)	0.1296 (2)	Cl	0.3277 (1)	0.31851 (8)	0.12318 (8)
P(1)	0.3471 (3)	0.1402 (2)	0.2654 (2)	P(1)	0.3411 (1)	0.13793 (7)	0.26432 (8)
P(2)	0.3164 (3)	0.3148 (2)	0.3741 (2	P(2)	0.3152 (1)	0.31114 (8)	0.37513 (8)
C(A1)	0.278 (1)	0.0421 (6)	0.3278 (7)	C(A1)	0.2714 (5)	0.0399 (3)	0.3285 (3)
C(A2)	0.202 (1)	−0.0241 (6)	0.2640 (7)	C(A2)	0.1953 (6)	−0.0273 (3)	0.2623 (4)
C(A3)	0.134 (2)	−0.0943 (7)	0.3072 (9)	C(A3)	0.1277 (6)	−0.0983 (3)	0.3081 (4)
C(A4)	0.141 (1)	−0.1019 (7)	0.4171 (8)	C(A4)	0.1368 (6)	−0.1047 (3)	0.4184 (4)
C(A5)	0.216 (1)	−0.0369 (7)	0.4820 (7)	C(A5)	0.2142 (6)	−0.0396 (4)	0.4846 (4)
C(A6)	0.284 (1)	0.0343 (7)	0.4395 (7)	C(A6)	0.2805 (5)	0.0321 (3)	0.4396 (3)
C(B1)	0.441 (1)	0.0921 (6)	0.1572 (7)	C(B1)	0.4304 (5)	0.0896 (3)	0.1539 (3)
C(B2)	0.386 (1)	0.1150 (8)	0.0495 (7)	C(B2)	0.3743 (6)	0.1096 (3)	0.0470 (4)
C(B3)	0.467 (2)	0.0771 (9)	−0.0287 (8)	C(B3)	0.4476 (7)	0.0738 (4)	−0.0346 (4)
C(B4)	0.589 (2)	0.0198 (8)	−0.0026 (9)	C(B4)	0.5753 (7)	0.0163 (4)	−0.0087 (4)
C(B5)	0.643 (2)	−0.0035 (8)	0.1025 (10)	C(B5)	0.6325 (7)	−0.0057 (4)	0.0971 (5)
C(B6)	0.565 (1)	0.0327 (8)	0.1826 (8)	C(B6)	0.5599 (6)	0.0304 (3)	0.1788 (4)
C(C1)	0.295 (1)	0.2885 (6)	0.5142 (6)	C(C1)	0.2963 (5)	0.2857 (3)	0.5164 (3)
C(C2)	0.408 (1)	0.3285 (7)	0.5974 (7)	C(C2)	0.4077 (6)	0.3240 (3)	0.5997 (4)
C(C3)	0.398 (1)	0.3092 (8)	0.7054 (7)	C(C3)	0.3988 (6)	0.3066 (4)	0.7072 (4)
C(C4)	0.283 (1)	0.2516 (9)	0.7303 (6)	C(C4)	0.2799 (6)	0.2500 (4)	0.7329 (3)
C(C5)	0.174 (1)	0.2125 (7)	0.6495 (7)	C(C5)	0.1705 (6)	0.2121 (4)	0.6513 (4)
C(C6)	0.182 (1)	0.2311 (7)	0.5411 (7)	C(C6)	0.1778 (5)	0.2296 (3)	0.5437 (3)
C(D1)	0.313 (1)	0.4340 (6)	0.3763 (6)	C(D1)	0.3153 (5)	0.4309 (3)	0.3783 (3)
C(D2)	0.401 (1)	0.4831 (7)	0.3136 (7)	C(D2)	0.4091 (6)	0.4795 (3)	0.3161 (4)
C(D3)	0.391 (1)	0.5721 (7)	0.3115 (8)	C(D3)	0.3980 (7)	0.5707 (3)	0.3145 (4)
C(D4)	0.290 (1)	0.6159 (6)	0.3720 (8)	C(D4)	0.2947 (7)	0.6124 (3)	0.3738 (4)
C(D5)	0.203 (1)	0.5669 (7)	0.4341 (8)	C(D5)	0.2033 (6)	0.5650 (3)	0.4362 (4)
C(D6)	0.214 (1)	0.4793 (7)	0.4378 (7)	C(D6)	0.2148 (6)	0.4748 (3)	0.4394 (4)
C(L1)	0.525 (1)	0.1807 (7)	0.3624 (7)	C(L1)	0.5227 (5)	0.1757 (3)	0.3610 (4)
C(L2)	0.529 (1)	0.2805 (6)	0.3720 (7)	C(L2)	0.5263 (5)	0.2757 (3)	0.3708 (3)
C(2)	−0.031 (1)	0.3241 (7)	0.1706 (7)	C(2)	−0.0523 (5)	0.3221 (3)	0.1614 (4)
C(M2)	−0.055 (2)	0.4138 (8)	0.1308 (10)	C(M2)	−0.0873 (8)	0.4116 (4)	0.1124 (5)
C(E2)	−0.113 (3)	0.4786 (13)	0.1932 (16)	C(E2)	−0.0794 (14)	0.4847 (5)	0.1865 (8)
C(3)	−0.013 (1)	0.2498 (8)	0.0978 (6)	C(3)	−0.0293 (4)	0.2481 (4)	0.0918 (3)
C(M3)	−0.025 (1)	0.2646 (9)	−0.032 (7)	C(M3)	−0.0455 (6)	0.2564 (5)	−0.0298 (4)
C(E3)	−0.181 (3)	0.2392 (18)	−0.0847 (12)	C(E3)	−0.2147 (9)	0.2408 (8)	−0.0875 (5)
B(4)	−0.002 (1)	0.1583 (10)	0.1527 (9)	B(4)	−0.0123 (6)	0.1587 (4)	0.1514 (4)
B(5)	−0.025 (1)	0.1794 (9)	0.2813 (9)	B(5)	−0.0307 (6)	0.1833 (4)	0.2823 (4)
B(6)	−0.040 (1)	0.2874 (8)	0.2869 (8)	B(6)	−0.510 (6)	0.2934 (4)	0.2816 (4)
B(7)	−0.161 (1)	0.2340 (8)	0.1817 (8)	B(7)	−0.1746 (6)	0.2288 (4)	0.1785 (4)
H(A2)	0.200 (11)	−0.022 (6)	0.189 (7)	H(A2)	0.195 (6)	−0.026 (4)	0.183 (4)
H(A3)	0.089 (11)	−0.143 (6)	0.267 (7)	H(A3)	0.077 (6)	−0.138 (4)	0.265 (4)
H(A4)	0.094 (11)	−0.154 (6)	0.448 (7)	H(A4)	0.084 (6)	−0.153 (4)	0.452 (4)
H(A5)	0.235 (11)	−0.040 (6)	0.558 (7)	H(A5)	0.228 (6)	−0.042 (4)	0.561 (4)
H(A6)	0.333 (10)	0.078 (6)	0.486 (6)	H(A6)	0.335 (6)	0.074 (3)	0.491 (4)
H(B2)	0.283 (11)	0.148 (6)	0.031 (7)	H(B2)	0.280 (6)	0.147 (4)	0.026 (4)
H(B3)	0.413 (12)	0.097 (7)	−0.105 (8)	H(B3)	0.412 (6)	0.092 (4)	−0.108 (4)
H(B4)	0.628 (12)	−0.006 (7)	−0.054 (7)	H(B4)	0.624 (6)	−0.004 (4)	−0.057 (4)
H(B5)	0.702 (12)	−0.044 (6)	0.124 (7)	H(B5)	0.711 (7)	−0.043 (4)	0.121 (4)
H(B6)	0.586 (10)	0.017 (6)	0.246 (6)	H(B6)	0.596 (6)	0.018 (4)	0.248 (4)
H(C2)	0.484 (11)	0.369 (6)	0.582 (7)	H(C2)	0.488 (6)	0.363 (4)	0.583 (4)
H(C3)	0.482 (11)	0.337 (6)	0.764 (7)	H(C3)	0.482 (6)	0.334 (4)	0.767 (4)
H(C4)	0.281 (10)	0.234 (6)	0.804 (6)	H(C4)	0.277 (6)	0.233 (4)	0.807 (4)
H(C5)	0.094 (11)	0.169 (6)	0.663 (7)	H(C5)	0.093 (6)	0.173 (4)	0.666 (4)
H(C6)	0.106 (11)	0.198 (6)	0.487 (7)	H(C6)	0.100 (6)	0.200 (3)	0.488 (4)
H(D2)	0.480 (12)	0.457 (6)	0.273 (7)	H(D2)	0.493 (6)	0.454 (4)	0.275 (4)
H(D3)	0.458 (11)	0.604 (6)	0.272 (7)	H(D3)	0.464 (6)	0.606 (4)	0.269 (4)
H(D4)	0.281 (11)	0.674 (6)	0.372 (6)	H(D4)	0.285 (6)	0.672 (4)	0.373 (4)
H(D5)	0.134 (11)	0.591 (6)	0.478 (7)	H(D5)	0.133 (6)	0.593 (4)	0.480 (4)
H(D6)	0.153 (12)	0.444 (6)	0.481 (7)	H(D6)	0.152 (6)	0.443 (4)	0.487 (4)
H(L11)	0.522 (10)	0.153 (5)	0.427 (6)	H(L11)	0.523 (6)	0.152 (3)	0.429 (4)
H(L12)	0.618 (10)	0.159 (6)	0.335 (6)	H(L12)	0.622 (6)	0.157 (4)	0.337 (4)
H(L21)	0.568 (9)	0.308 (5)	0.312 (6)	H(L21)	0.570 (6)	0.309 (4)	0.311 (4)
H(L22)	0.599 (10)	0.291 (5)	0.435 (6)	H(L22)	0.604 (6)	0.290 (3)	0.438 (4)
H(M21)	−0.189 (13)	0.411 (7)	0.071 (8)	H(M21)	−0.198 (7)	0.412 (4)	0.069 (5)
H(M22)	−0.000 (14)	0.430 (8)	0.074 (9)	H(M22)	−0.014 (7)	0.429 (4)	0.066 (5)
H(E21)	−0.149 (14)	0.538 (8)	0.156 (9)	H(E21)	−0.149 (8)	0.539 (5)	0.163 (5)
H(E22)	0.027 (19)	0.491 (11)	0.216 (12)	H(E22)	0.028 (8)	0.498 (5)	0.213 (5)
H(E23)	−0.113 (20)	0.467 (10)	0.249 (12)	H(E23)	−0.123 (8)	0.463 (5)	0.257 (5)
H(M31)	0.000 (12)	0.201 (6)	−0.069 (7)	H(M31)	0.007 (7)	0.205 (4)	−0.065 (4)
H(M32)	0.005 (12)	0.316 (7)	−0.039 (7)	H(M32)	−0.007 (7)	0.311 (4)	−0.049 (4)
H(E31)	−0.237 (16)	0.267 (10)	−0.165 (10)	H(E31)	−0.246 (8)	0.264 (5)	−0.167 (5)
H(E32)	−0.297 (16)	0.263 (10)	−0.050 (10)	H(E32)	−0.300 (8)	0.267 (5)	−0.045 (5)
H(E33)	−0.221 (19)	0.170 (11)	−0.082 (12)	H(E33)	−0.234 (8)	0.177 (5)	−0.086 (5)
H(4)	−0.000 (10)	0.092 (6)	0.099 (7)	H(4)	−0.000 (6)	0.088 (4)	0.104 (4)

Table VIII (Continued)

2				3			
atom	x	y	z	atom	x	y	z
H(5)	−0.032 (10)	0.132 (6)	0.348 (6)	H(5)	−0.034 (6)	0.133 (3)	0.352 (4)
H(6)	−0.082 (10)	0.328 (6)	0.344 (6)	H(6)	−0.095 (6)	0.331 (4)	0.344 (4)
H(7)	−0.310 (10)	0.238 (6)	0.148 (6)	H(7)	−0.317 (5)	0.238 (4)	0.145 (4)

Table IX. Bond Distances (Å) in 2 and 3

	2 (M = Co)	3 (M = Fe)
M–Cl	2.292 (2)	2.270 (1)
M–P(1)	2.203 (2)	2.246 (1)
M–P(2)	2.203 (2)	2.261 (1)
M–C(2)	2.085 (9)	2.164 (5)
M–C(3)	2.092 (7)	2.136 (4)
M–B(4)	2.146 (12)	2.138 (6)
M–B(5)	2.156 (11)	2.147 (6)
M–B(6)	2.096 (10)	2.146 (6)
P(1)–C(A1)	1.831 (8)	1.841 (5)
P(1)–C(B1)	1.830 (8)	1.834 (5)
P(1)–C(L1)	1.854 (10)	1.861 (5)
P(2)–C(C1)	1.839 (7)	1.846 (5)
P(2)–C(D1)	1.825 (9)	1.834 (5)
P(2)–C(L2)	1.847 (9)	1.845 (5)
C(A1)–C(A2)	1.376 (12)	1.404 (7)
C(A1)–C(A6)	1.397 (11)	1.387 (7)
C(A2)–C(A3)	1.369 (12)	1.391 (7)
C(A3)–C(A4)	1.374 (13)	1.376 (8)
C(A4)–C(A5)	1.367 (13)	1.384 (9)
C(A5)–C(A6)	1.377 (13)	1.390 (7)
C(B1)–C(B2)	1.395 (11)	1.377 (7)
C(B1)–C(B6)	1.374 (12)	1.401 (7)
C(B2)–C(B3)	1.405 (13)	1.389 (8)
C(B3)–C(B4)	1.340 (15)	1.374 (9)
C(B4)–C(B5)	1.367 (15)	1.374 (10)
C(B5)–C(B6)	1.399 (13)	1.388 (8)
C(C1)–C(C2)	1.420 (11)	1.402 (7)
C(C1)–C(C6)	1.372 (11)	1.392 (7)
C(C2)–C(C3)	1.403 (11)	1.388 (7)
C(C3)–C(C4)	1.373 (13)	1.392 (9)
C(C4)–C(C5)	1.378 (13)	1.377 (8)
C(C5)–C(C6)	1.401 (11)	1.386 (7)
C(D1)–C(D2)	1.382 (11)	1.405 (7)
C(D1)–C(D6)	1.402 (11)	1.397 (7)
C(D2)–C(D3)	1.365 (13)	1.400 (8)
C(D3)–C(D4)	1.397 (14)	1.382 (9)
C(D4)–C(D5)	1.369 (14)	1.384 (9)
C(D5)–C(D6)	1.345 (13)	1.385 (8)
C(L1)–C(L2)	1.532 (13)	1.537 (7)
C(2)–C(M2)	1.464 (14)	1.509 (8)
C(2)–C(3)	1.480 (13)	1.464 (8)
C(2)–B(6)	1.575 (13)	1.568 (8)
C(2)–B(7)	1.771 (14)	1.788 (9)
C(M2)–C(E2)	1.398 (20)	1.449 (13)
C(3)–C(M3)	1.520 (10)	1.513 (6)
C(3)–B(4)	1.557 (17)	1.554 (8)
C(3)–B(7)	1.761 (11)	1.781 (7)
C(M3)–C(E3)	1.445 (18)	1.488 (9)
B(4)–B(5)	1.687 (14)	1.717 (8)
B(4)–B(7)	1.839 (16)	1.800 (9)
B(5)–B(6)	1.660 (16)	1.694 (10)
B(5)–B(7)	1.748 (15)	1.756 (9)
B(6)–B(7)	1.723 (14)	1.805 (9)
⟨C–H⟩	0.98	0.97
⟨B–H⟩	1.16	1.15

ening. The Fe–P bond lengths, on the other hand, show an opposite trend, in line with the larger radius of iron compared to that of cobalt; in both molecules, the M–P distances are within the range observed in other first-row transition-metal–diphos complexes.[15,22] In both **2** and **3**, the Cl–M–P and P–M–P angles are close to 90°, consistent with quasi-octahedral hybridization on the metal atoms. The diphos ligands in each case are normal, and all phenyl rings are planar within experimental error.

An unusual feature of these structures is their adoption of the chiral space group $P2_1$. Although **2** and **3** are optically inactive in solution, their enantiomers crystallize separately and hence are resolvable by physical means.

Experimental Section

Materials. 2,3-Diethyl-2,3-dicarbahexaborane(8), $(C_2H_5)_2C_2B_4H_6$, was prepared by a modification of the synthesis described elsewhere.[4] In the present work, the entire amounts of the three reagents were combined initially, using the same quantities as before,[4] instead of being added in small increments as in the earlier procedure.[4] 3-Hexyne was degassed in vacuo at −196 °C, and pentaborane(9) and triethylamine were condensed at −196 °C into the reactor, which was then placed in a 0 °C bath and stirred for 3 days (while allowing the bath to warm slowly to room temperature). Workup of the product was carried out as before, and all other details were unchanged from the earlier procedure.[4] This modified method produces smaller yields of carborane (~25–30%) but is a simpler and easier procedure. The 3-hexyne (Farchan Chemical) and pentaborane(9), B_5H_9 (U.S. Government stockpile), were used as received. Triethylamine was dried over 4-Å molecular sieve and distilled in vacuo before use. Cobalt(II) chloride was dried at high temperature in vacuo and stored in a moisture-free desiccator. Anhydrous $FeCl_2$ and 1,2-bis(diphenylphosphino)ethane (diphos) were used as received and stored in a nitrogen-filled drybox. Sodium hydride (50% oil) was washed twice with hexane before use. Tetrahydrofuran was dried over $LiAlH_4$ or dried over and distilled from Na/benzophenone under N_2. Diethyl ether was dried over and distilled from $LiAlH_4$ under vacuum. All other solvents were distilled and stored over 4-Å molecular sieve, and all solvents were degassed before use. All other chemicals were reagent grade and were used as received. Column chromatography employed silica gel 60 (Merck), and thin-layer chromatography was conducted on precoated glass plates (silica gel F-254) or on Eastman Chromagram sheets (silica).

Instrumentation. Pulse Fourier transform ^{11}B (115 MHz), ^1H (360 MHz) and ^{31}P (146 MHz) NMR spectra were recorded on a Nicolet NT-360 spectrometer equipped with a 1180E/293B data processor. Broad-band heteronuclear decoupling was used in obtaining the ^{11}B and ^{31}P NMR spectra. Infrared spectra were recorded on a Perkin-Elmer 1430 ratio recording spectrophotometer in KBr pellets or 1-mm NaCl solution cells. Ultraviolet spectra were obtained on a Varian Cary 17D spectrophotometer from 700 to 215 nm. EPR spectra were recorded on a Varian E-line spectrometer using a weak-pitch Varian standard. Unit resolution mass spectra (EI) were recorded on a VG-70/70H mass spectrometer (Harvey Laboratories, Charlottesville, VA) or on a Finnigan MAT-4500 GC/MS spectrometer using perfluorotributylamine (FC43) as a peak-matching standard. All new compounds reported exhibited mass spectra containing parent groupings characteristic of the indicated composition, as determined by calculated spectra on the basis of natural isotope distributions. Manipulation and storage of air-sensitive compounds were conducted in gloveboxes in an O_2-free atmosphere or in a Schlenk-type apparatus by using standard techniques. Magnetic measurements were made on a SHE Corp. 905 superconducting magnetometer/susceptometer.

Synthesis of 1,2,3-$(Ph_3P)(Br)Ni(Et_2C_2B_4H_3$-5-$PPh_3)$ (1). A THF solution of $Na^+Et_2C_2B_4H_5^-$ was prepared from 0.283 g (2.15 mmol) of $Et_2C_2B_4H_6$ and 0.081 g (3.38 mmol) of NaH in 25 mL of dry THF. The carborane solution was filtered in vacuo into a reaction flask containing 1.600 g of $(Ph_3P)_2NiBr_2$ (2.15 mmol) cooled in liquid nitrogen. An additional 25 mL of dry THF was transferred into the reaction flask, and the contents were allowed to thaw. The mixture was stirred at room temperature for $2^1/_2$ days, after which the solvent was removed in vacuo and the dark brown residue was taken into an O_2-free drybox. The residue was dissolved in a minimum amount of CH_2Cl_2, and the solution was placed on a 5 cm × 20 cm silica gel column charged with *n*-hexane. A brown band consisting of many minor products was eluted with CH_2Cl_2/*n*-hexane (3:1). Elution with CH_2Cl_2 gave a purple band, which on removal of solvent in vacuo afforded purple solid **1**, 0.460 g (0.581 mmol), 27.1% based on carborane employed. Compound **1** is air-stable as a solid, but is moderately air-sensitive in polar solvents and more so in nonpolar solvents. The UV–visible spectrum contains a maximum at

(22) (a) Churchill, M. R.; O'Brien, T. A. *J. Chem. Soc. A* **1970**, 206. (b) Davis, R. E.; Riley, P. E. *Inorg. Chem.* **1980**, *19*, 674. (c) Riley, P. E.; Capshew, C. E.; Pettit, R.; Davis, R. E. *Ibid.* **1978**, *17*, 408. (d) Kaduk, J. A.; Ibers, J. A. *Ibid.* **1977**, *16*, 3283.

Table X. Selected Bond Angles (deg) for **2** and **3**

	2 (M = Co)	**3** (M = Fe)		**2** (M = Co)	**3** (M = Fe)
Cl-M-P(1)	91.13 (8)	92.96 (5)	C(B2)-C(B3)-C(B4)	122.2 (10)	119.70 (6)
Cl-M-P(2)	87.52 (8)	89.18 (5)	C(B3)-C(B4)-C(B5)	121.3 (9)	120.80 (6)
Cl-M-C(2)	94.7 (3)	95.11 (15)	C(B4)-C(B5)-C(B6)	118.1 (10)	119.50 (6)
Cl-M-C(3)	89.5 (2)	90.04 (13)	C(B1)-C(B6)-C(B5)	121.2 (9)	120.40 (6)
Cl-M-B(4)	118.0 (3)	119.00 (2)	P(2)-C(C1)-C(C2)	116.7 (6)	118.30 (4)
Cl-M-B(5)	163.0 (3)	164.30 (2)	P(2)-C(C1)-C(C6)	123.7 (6)	123.00 (4)
Cl-M-B(6)	133.4 (3)	130.60 (2)	C(C2)-C(C1)-C(C6)	119.6 (7)	118.60 (4)
P(1)-M-P(2)	86.96 (8)	84.10 (5)	C(C1)-C(C2)-C(C3)	118.5 (8)	120.40 (4)
P(1)-M-C(2)	162.1 (3)	160.25 (16)	C(C2)-C(C3)-C(C4)	120.8 (8)	120.00 (5)
P(1)-M-C(3)	121.8 (3)	122.40 (2)	C(C3)-C(C4)-C(C5)	120.6 (7)	119.70 (5)
P(1)-M-B(4)	87.7 (4)	88.20 (2)	C(C4)-C(C5)-C(C6)	119.5 (8)	120.70 (5)
P(1)-M-B(5)	94.0 (3)	93.90 (2)	C(C1)-C(C6)-C(C5)	121.0 (8)	120.50 (5)
P(1)-M-B(6)	135.0 (3)	135.80 (2)	P(2)-C(D1)-C(D2)	121.7 (7)	121.00 (4)
P(2)-M-C(2)	110.2 (3)	113.97 (16)	P(2)-C(D1)-C(D6)	120.9 (7)	119.70 (4)
P(2)-M-C(3)	151.2 (3)	153.50 (2)	C(D2)-C(D1)-C(D6)	117.3 (8)	119.20 (5)
P(2)-M-B(4)	154.0 (3)	151.20 (2)	C(D1)-C(D2)-C(D3)	121.2 (9)	119.60 (5)
P(2)-M-B(5)	108.9 (3)	105.50 (2)	C(D2)-C(D3)-C(D4)	102.6 (9)	119.90 (6)
P(2)-M-B(6)	88.7 (3)	88.70 (2)	C(D3)-C(D4)-C(D5)	118.0 (9)	120.80 (5)
M-P(1)-C(A1)	117.7 (3)	118.42 (15)	C(D4)-C(D5)-C(D6)	121.7 (10)	119.80 (6)
M-P(1)-C(B1)	120.6 (3)	118.50 (2)	C(D1)-C(D6)-C(D5)	121.2 (9)	120.60 (6)
M-P(1)-C(L1)	106.9 (3)	108.96 (16)	P(1)-C(L1)-C(L2)	113.0 (7)	111.30 (4)
C(A1)-P(1)-C(B1)	101.1 (4)	101.40 (2)	P(2)-C(L2)-C(L1)	106.0 (7)	106.80 (3)
C(A1)-P(1)-C(L1)	105.5 (4)	104.40 (2)	M-C(2)-C(M2)	133.7 (8)	135.10 (4)
C(B1)-P(1)-C(L1)	103.3 (4)	103.30 (2)	M-C(2)-B(7)	91.1 (5)	90.30 (3)
M-P(2)-C(C1)	123.5 (3)	125.57 (16)	C(M2)-C(2)-C(3)	122.1 (9)	119.70 (5)
M-P(2)-C(D1)	117.1 (3)	115.48 (16)	C(M2)-C(2)-B(6)	128.7 (9)	128.00 (6)
M-P(2)-C(L2)	104.0 (3)	104.10 (15)	C(M2)-C(2)-B(7)	135.1 (8)	134.40 (5)
C(C1)-P(2)-C(D1)	101.6 (4)	100.90 (2)	C(3)-C(2)-B(6)	108.8 (8)	112.10 (5)
C(C1)-P(2)-C(L2)	101.3 (4)	101.70 (2)	C(2)-C(M2)-C(E2)	121.0 (1)	117.00 (7)
C(D1)-P(2)-C(L2)	107.5 (4)	107.30 (2)	M-C(3)-C(M3)	135.5 (6)	136.10 (3)
P(1)-C(A1)-C(A2)	120.1 (6)	118.80 (4)	M-C(3)-B(7)	91.2 (4)	91.40 (3)
P(1)-C(A1)-C(A6)	122.5 (7)	122.80 (4)	C(2)-C(3)-C(M3)	120.4 (1)	122.50 (6)
C(A2)-C(A1)-C(A6)	117.1 (8)	118.30 (5)	C(2)-C(3)-B(4)	115.0 (7)	113.90 (4)
C(A1)-C(A2)-C(A3)	121.8 (8)	120.10 (5)	C(M3)-C(3)-B(4)	124.3 (10)	123.00 (6)
C(A2)-C(A3)-C(A4)	120.9 (9)	120.90 (5)	C(M3)-C(3)-B(7)	133.2 (7)	132.50 (4)
C(A3)-C(A4)-C(A5)	118.2 (9)	119.50 (5)	C(3)-C(M3)-C(E3)	113.1 (10)	113.10 (5)
C(A4)-C(A5)-C(A6)	121.4 (8)	120.00 (5)	M-B(4)-B(7)	87.3 (6)	90.80 (3)
C(A1)-C(A6)-C(A5)	120.5 (9)	121.20 (5)	C(3)-B(4)-B(5)	104.0 (9)	104.50 (5)
P(1)-C(B1)-C(B2)	120.4 (7)	122.10 (4)	M-B(5)-B(7)	89.4 (6)	91.70 (3)
P(1)-C(B1)-C(B6)	119.5 (7)	119.10 (4)	B(4)-B(5)-B(6)	104.6 (9)	103.80 (5)
C(B2)-C(B1)-C(B6)	120.1 (8)	118.80 (5)	M-B(6)-B(7)	92.1 (6)	90.40 (3)
C(B1)-C(B2)-C(B3)	117.0 (9)	120.70 (5)	C(2)-B(6)-B(5)	107.5 (8)	105.60 (5)

475 nm (CH_3CN), 540 nm (CH_3OH), 540 nm (dimethylformamide), or 545 nm (hexane).

Crystals suitable for X-ray studies were obtained by evaporation of a methanol solution of **1** under an N_2 atmosphere.

Synthesis of 1,2,3-$(Ph_2PCH_2)_2(Cl)Co(Et_2C_2B_4H_4)$ (2). Into a tipping storage tube (Figure 4, tube A) was placed 0.788 g (6.00 mmol) of 2,3-$Et_2C_2B_4H_6$, which was degassed and evacuated. Into reaction flask C were placed a Teflon-coated spin bar, 0.794 g (6.12 mmol) of anhydrous $CoCl_2$, and 2.38 g (5.97 mmol) of $(Ph_2PCH_2)_2$. Side-arm flask B was charged with 0.169 g of NaH (7.04 mmol) along with a spin bar. The setup was assembled as in Figure 4, attached to a vacuum line, and evacuated. Flask B was cooled in liquid nitrogen (−196 °C), and 35 mL of THF was distilled into the flask. Storage tube A was turned 180° and its stopcock opened to empty the contents into the reaction flask. After transfer of the contents, the storage tube was isolated from the rest of the system. Side-arm flask B was allowed to warm to room temperature, and its contents were stirred, during which evolution of H_2 was observed. After effervescence ceased (approximately 45 min), the flask was recooled in liquid nitrogen and the H_2 evacuated. The flask was again warmed to room temperature, and its contents were stirred for 5 min, after which the contents of the flask were refrozen and any hydrogen present was evacuated. This procedure of warming and freezing the contents of the flask was continued until no more hydrogen gas was evolved. The entire setup was then isolated from the vacuum line. Flask B was rewarmed to room temperature, and the contents were filtered through frit D into flask C (maintained at −196 °C). Flask C was isolated, flask B was immersed in liquid nitrogen, and 30 mL of THF was condensed into the latter flask, which was warmed to room temperature and the mixture stirred for 5 min. The THF was then poured onto frit D and allowed to stand on the frit for 5 min. At the end of this time, the THF was filtered into flask C, which was again isolated and allowed to warm to room temperature. The contents of the flask were stirred, during which the mixture became greenish brown after about 5 min. The solution became darker brown on continued stirring and maintained that color for the reaction period. The reaction was stirred for 4–12 h, at the end of which the contents of the flask were placed under N_2 and opened to the air. The THF was removed by rotary evaporation, and the reaction mixture was then placed in a minimum amount of CH_2Cl_2 that allowed it to be completely transferred by pipet. Some solid was also inadvertently transferred. The reaction mixture was placed atop a 5 × 30 cm silica gel column packed in hexane. Elutions were made successively with 100-mL portions of hexane, 25%, 50%, and 75% CH_2Cl_2/hexane, and

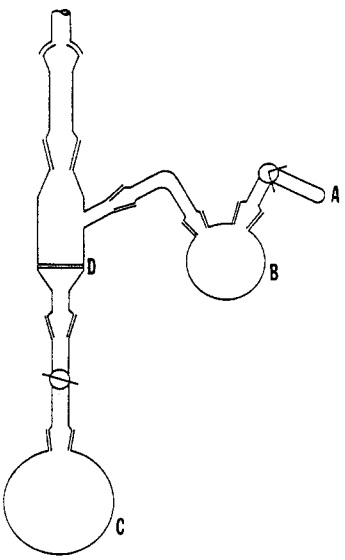

Figure 4. Apparatus for synthesis of **2** and **3**.

finally CH_2Cl_2. A pink oil (20 mg) of unknown composition was eluted with 25% CH_2Cl_2. Elution with CH_2Cl_2 gave a brown solution, which on rotary evaporation gave a brown solid. Thin-layer chromatography of the brown band in 50% CH_2Cl_2/hexane gave primarily 1,2,3-$(Ph_2PCH_2)_2(Cl)Co(Et_2C_2B_4H_4)$ (**2**): R_f 0.32; mol wt 622.2; yield 530 mg (14.2%), UV-visible maxima (CH_2Cl_2): 461 and 260 nm. ^{31}P NMR (146 MHz), proton decoupled, in 1:1 $CDCl_3/CH_2Cl_2$: singlet, δ 67.47 relative to H_3PO_4.

Several other bands were observed during the TLC of **2**, but the largest of these amounted to less than 2 mg of product and they were not identified.

Synthesis of 1,2,3-$(Ph_2PCH_2)_2(Cl)Fe(Et_2C_2B_4H_4)$ (3). Via the procedure employed in the preparation of **2**, described above, a solution of $Na^+Et_2C_2B_4H_5^-$ in 30 mL of THF, prepared from 0.0907 g (0.690 mmol) of $Et_2C_2B_4H_6$, was reacted with 0.186 g (1.47 mmol) of $FeCl_2$ and 0.413 g (1.04 mmol) of $(Ph_2PCH_2)_2$ for a period of 4–15 h at room temperature, producing an orange-red solution. After removal of solvent, the mixture was dissolved in a minimum volume of CH_2Cl_2 and chromatographed on a 5 × 30 cm silica gel column packed in hexane. Elution with 50% acetone/hexane gave a red-orange solution, which after rotary evaporation gave a red solid. Thin-layer chromatography of the red solid in 50% CH_2Cl_2/hexane gave 1,2,3-$(Ph_2PCH_2)_2(Cl)Fe(Et_2C_2B_4H_4)$ (**3**): R_f 0.44; mol wt 619.2; yield 68 mg (16%). UV-visible maxima (CH_2Cl_2): 460 and 261 nm.

Reaction of 2 with CH_3MgI. A solution of the Grignard CH_3MgI was prepared from 2.5 mL of CH_3I and 25 mL of anhydrous ether and added under N_2 to an excess of Mg turnings and the mixture stirred for 30 min at room temperature. A diethyl ether solution of **2** (0.12 g, 0.019 mmol) was added to the CH_3MgI solution via a syringe fitted with a double-ended stainless-steel needle and the mixture stirred for 30 min, after which the solution was then poured over a small amount of ice to eliminate any excess Grignard reagent. The resulting water/ether mixture was placed in a separatory funnel and the ether layer removed, after which Na_2SO_4 was added to the ether solution to remove any water still present. The Na_2SO_4 was filtered off and the resulting brown solution rotary-evaporated. Thin-layer chromatography of this solution in 50% dichloromethane/hexane gave 1,2,3-$(Ph_2PCH_2)_2(I)Co(Et_2C_2B_4H_4)$ (**5**): R_f 0.6; mol wt 713.7; yield 28.5 mg (21%). UV-visible maxima (CH_2Cl_2): 475 and 253 nm. ^{31}P NMR (vide supra): singlet, δ 75.42 relative to H_3PO_4.

Reaction of 2 with KCN in Refluxing Methanol. A mixture of **2** (0.036 g, 0.058 mmol) and 0.130 g of KCN (2.00 mmol) was placed under nitrogen in a round-bottom flask fitted with a water-cooled condenser and nitrogen inlet. The system was purged for 5 min, and 30 mL of methanol was added. The flask was placed in a heating mantle and refluxed for 10 min with stirring. The solution during this time changed color from brown to yellow. The solution was cooled, exposed to the air, and rotary evaporated. The yellow oil was dissolved in a minimum of dichloromethane and placed on a 2 × 15 cm silica gel column packed in hexane. Elution of the column with 80% methylene chloride/acetone gave a yellow band. Thin-layer chromatography of this band in 96% methylene chloride/acetone gave 1,2,3-$(Ph_2PCH_2)_2(CN)Co(Et_2C_2B_4H_4)$ (**4**): R_f 0.66; mol wt 612.8; yield 7.1 mg (20%). UV-visible maxima (CH_2Cl_2): 362 and 257 nm. ^{31}P NMR (vide supra): singlet, δ 73.21 relative to H_3PO_4.

Reaction of 2 with KCN at Room Temperature. A sample of **2** (0.022 g, 0.035 mmol) and 0.021 g of KCN (0.32 mmol) were stirred in 70 mL of methanol at room temperature for 10 h. The resulting solution was evaporated to give a brown solid, which was thin-layer chromatographed in CH_2Cl_2 to give a brown moving band and a yellow nonmoving band. The yellow band was extracted with acetone, dried, and chromatographed in 96% methylene chloride/acetone to give **4**: R_f 0.66; yield 2.4 mg (11%).

Attempted Reaction of 2 with NaH. A 0.0432-g sample of **2** in THF (0.069 mmol) was added to 0.100 g of NaH (4.02 mmol) under nitrogen with standard Schlenk techniques. The resulting mixture was stirred for 12 h at room temperature, filtered, and rotary-evaporated. Thin-layer chromatography in 50% CH_2Cl_2/hexane gave one brown band, which was identified by mass spectrometry as **2**.

Attempted Reaction of 3 with NaH. A THF solution containing 0.0125 g of **3** (0.02 mmol) was added to 0.1 g of NaH (4.17 mmol) under nitrogen and stirred for 2 h. The reaction mixture was passed through a fritted filter, opened to the air, rotary-evaporated, and chromatographed in 50% methylene chloride/hexane to give one red band, which was identified from its infrared spectrum and R_f value as **3**.

Attempted Reaction of 2 with CH_3CN in Methanol. A 0.02-g sample of **2** (0.03 mmol) and 0.01 g of NH_4PF_6 (0.061 mmol) were placed in a solution consisting of 10 mL of methanol and 1 mL of CH_3CN under nitrogen. Compound **2** was insoluble in this mixture, so dichloromethane was added until the solid dissolved (approximately 2 mL). The mixture was stirred at room temperature for 4 h and then rotary-evaporated to dryness. Thin-layer chromatography of the resulting solid in 50% dichloromethane/hexane gave only one band, which was identified from its R_f value as **2**.

X-ray Structure Determinations on 1, 2, and 3. Single crystals of each compound were grown by slow evaporation from methanol (for **1**) or hexane/dichloromethane (for **2** and **3**). In each case, crystals were examined under the polarizing microscope and found acceptable; these were mounted on glass fibers in random orientations. Precession photography was employed to identify crystals satisfactory for data collection. Relevant crystal data and experimental parameters are listed in Table IV. For **1** and **3**, cell dimensions and space group data were obtained by standard methods on an Enraf-Nonius four-circle diffractometer. The θ–2θ scan technique was used as previously described[23] to record the intensities for all nonequivalent reflections within the ranges of θ given in Table IV. Scan widths were calculated as $(A + B \tan \theta)$, where A is estimated from the mosaicity of the crystal and B allows for the increase in peak width due to $K\alpha_1$–$K\alpha_2$ splitting.

The intensities of three standard reflections showed no greater fluctuations during data collection than those expected from the Poisson statistics. The raw intensity data were collected for Lorentz–polarization effects and absorption. Only those reflections for which $F_o^2 > 3\sigma(F_o^2)$, where $\sigma(F_o^2)$ was estimated from counting statistics ($p = 0.03$),[24] were used in the final refinement of the structural parameters.

Solution and Refinement of the Structures. For **1** and **3**, three-dimensional Patterson syntheses were used to determine the heavy-atom positions, which phased the data sufficiently well to permit location of the remaining nonhydrogen atoms from Fourier syntheses. Full-matrix least-squares refinement was carried out as previously described.[23] Anisotropic temperature factors were introduced for the nonhydrogen atoms. Additional Fourier difference functions permitted location of the nonmethyl hydrogen atoms, which were included for four cycles of least-squares refinement and then held fixed. In the case of **3**, the absolute configuration was determined by comparing the refinement with that of the mirror image configuration (the configuration reported resulted in a lower R factor by 0.02).

For compound **2**, approximate cell dimensions, an orientation matrix for data collection, and the space group were obtained on a Nicolet P_3m diffractometer by using techniques similar to those employed for **3**. Since **2** was found to be isomorphous with **3**, no Patterson synthesis was necessary. Instead, the initial atomic positions for **2** were taken from those already determined for **3**; full-matrix least-squares refinement was then conducted as for **2**.

The models converged to the R values given in Table IV. Final difference Fourier maps were featureless. Listings of the observed and calculated structure factors are available together with thermal parameters as supplementary material.

Acknowledgment. This work was supported by the U.S. Army Research Office and the National Science Foundation. We thank Drs. T. L. Venable and J. T. Spencer for recording the NMR spectra, Dr. R. Butcher of Howard University for collecting X-ray data on compound **2**, Teresa Rowe for the magnetic moment measurements, and Dr. Odatt Rajan for the ESR spectra.

Registry No. **1**, 98360-71-5; **2**, 98330-39-3; **3**, 98330-40-6; **4**, 98330-41-7; **5**, 98330-42-8; $(Ph_3P)_2NiBr_2$, 14126-37-5.

Supplementary Material Available: Tables of calculated and observed structure factors, thermal parameters, and mean planes (63 pages). Ordering information is given on any current masthead page.

(23) Freyberg, D. P.; Mockler, G. M.; Sinn, E. *J. Chem. Soc., Dalton Trans.* **1976**, 447.
(24) Corfield, P. W. R.; Doedens, R. J.; Ibers, J. A. *Inorg. Chem.* **1967**, *6*, 197.